

# Fluorescence switching method for cascade detection of salicylaldehyde and zinc(II) ion using protein protected gold nanoclusters



Xi Liu <sup>a,b</sup>, Changhui Fu <sup>a</sup>, Xiangling Ren <sup>a</sup>, Huiyu Liu <sup>a,\*</sup>, Linlin Li <sup>a,\*</sup>, Xianwei Meng <sup>a</sup>

<sup>a</sup> Laboratory of Controllable Preparation and Application of Nanomaterials, Center for Micro/nanomaterials and Technology, Technical Institute of Physics and Chemistry, Chinese Academy of Sciences, No. 29, Zhongguancun, East Road, Beijing 100190, People's Republic of China

<sup>b</sup> University of Chinese Academy of Sciences, Beijing 100049, People's Republic of China

## ARTICLE INFO

### Article history:

Received 7 April 2015

Received in revised form

3 June 2015

Accepted 15 June 2015

Available online 23 June 2015

### Keywords:

Gold nanoclusters

Salicylaldehyde

Zn<sup>2+</sup>

Schiff base

Fluorescence switching

Coordination

## ABSTRACT

A new fluorescence switching sensor for cascade detection of salicylaldehyde (SA) and Zinc(II) ion was developed based on bovine serum albumin protected gold nanoclusters (BSA-AuNCs). In the detection, SA interacted with amino groups of BSA-AuNCs, inducing simultaneous formation of fluorescent Schiff base and fluorescence quenching of AuNCs. Zn(II) could further strongly coordinate with the Schiff base ligands, leading to blue-shift and increase of the fluorescence from Schiff base–metal coordination complexes and simultaneous recovery of fluorescence from AuNCs. The new fluorescence switching sensor for Zn<sup>2+</sup> detection has advantages of simplicity, rapidity, naked-eye detection, high sensitivity and selectivity. The linear range of the method for Zn<sup>2+</sup> detection is from 0.1 μM to 100 μM with the limit of detection (LOD) of 29.28 nM. In practical samples, the recoveries of the samples ranged from 99.63% to 100.58%.

© 2015 Elsevier B.V. All rights reserved.

## 1. Introduction

As the second most abundant essential trace element in human body (Huang et al., 2013), zinc ion (Zn<sup>2+</sup>) widely distributes in cells and body fluids. It plays a basic mediation role in lots of physiological processes including regulation of gene expression and cellular apoptosis, as co-factors in metalloenzyme catalysis and neurotransmission (Wang et al., 2013). Disorders of zinc ion metabolism would cause kinds of serious neurological diseases such as Alzheimer's, Parkinson's disease, cerebral ischemia and epilepsy (Kim, K.B., et al., 2013; Takeda, 2001). Thus, it is significantly important to design biosensors for the detection of Zn<sup>2+</sup> with high selectivity, sensitivity and reliability (Jung et al., 2009; Lee et al., 2011, 2012; Zhou et al., 2011).

Zn<sup>2+</sup> is a d-block metal ion. It comprises a closed shell electronic structure of 3d<sup>10</sup> without oxidation-reduction activity in biological environments that makes the detection of Zn<sup>2+</sup> difficult (Wang et al., 2013). In addition, the conventional detection techniques such as electronic absorption spectroscopy, electron paramagnetic resonance (EPR) and nuclear magnetic resonance (NMR) are not effective for Zn<sup>2+</sup> ion which is silent to the spectrum. Other conventional techniques such as ion selective electrodes

(ISE) and atomic absorption spectrometry (AAS) always require expensive equipment. In recent years, fluorescent chemical sensors have been applied for metal ions detection with advantages of high sensitivity, high selectivity and easiness of use (Shahid et al., 2012), enabling real-time dynamic testing and targeting detection of metal ions (Chen et al., 2008; Swamy et al., 2010). The fluorescent chemical sensors for the detection of Zn<sup>2+</sup> generally contain fluorophores and their derivatives, such as coumarin (Kim, J. H., et al., 2013; Lee et al., 2006), anthracene and quinolone (Ding et al., 2011; Jiang et al., 2011; Liu et al., 2009; Maity and Govindaraju, 2012; Park et al., 2011). It is known that Schiff base derivatives incorporating a fluorescent moiety could form strong coordinating bonds with transition metal ions, yield stable and intense fluorescent metal complexes, and hence be utilized for optical detection of transition metal ions including zinc ion (Cozzi, 2004; Gupta et al., 2013; Joseph et al., 2010; Kim, K.B., et al., 2013; Xu et al., 2010). Nevertheless, synthesis of these Schiff base derivatives generally requires complicated steps, strict experimental conditions and expensive chemicals. Some of the Zn<sup>2+</sup> sensors suffer from interference of some heavy metal ions and other transition metal ions such as Cu<sup>2+</sup> (Sheng et al., 2008).

As a new-emerged class of nanomaterials, ultrasmall gold nanoclusters (AuNCs) have unique optical properties (Xu and Suslick, 2010; Zheng et al., 2007). When the size of AuNCs decreases to comparable to the Fermi wavelength (< 1 nm) of an electron, they exhibit fluorescent characteristics due to the quantum size effect

\* Corresponding authors. Fax: +86 10 82543521.

E-mail addresses: liuhu@mail.ipc.ac.cn (H. Liu), linlinli@mail.ipc.ac.cn (L. Li), mengxw@mail.ipc.ac.cn (X. Meng).

(Zheng et al., 2007). Compared to semiconductor quantum dots and transition metal ion-doped nanoparticles, gold nanoclusters process excellent properties, such as green chemical synthesis, size-dependent emission, low toxicity and anti-photobleaching (Albrecht et al., 2012; Diez and Ras, 2011). Recently, AuNCs have been successfully applied in fluorescent detection of metal ions, small biomolecules, and nucleic acids (Adhikari and Banerjee, 2010; Chen et al., 2010; Lin and Tseng, 2010; Tu et al., 2011). For example, Ying et al. demonstrated the bovine serum albumin (BSA) stabilized gold nanoclusters were capable of sensing  $Hg^{2+}$  (Xie et al., 2010). Glutathione-capped gold nanoclusters have been used the detection of  $Cu^{2+}$  (Chen et al., 2009). Human serum albumin (HSA) stabilized gold nanoclusters have been applied for the detection of free bilirubin in blood serum as fluorometric and colorimetric probe (Santhosh et al., 2014). A colorimetric detection system for glucose was developed based on the peroxidase-like activity of apoferritin paired gold clusters (Jiang et al., 2015). However, to the best of our knowledge, the detection of zinc ion via AuNCs has been rarely reported. Meanwhile, SA is a constituent of buckwheat groats and *Filipendula vulgaris*. SA as a natural species shows remarkable inhibition effects on the growth of certain species of bacteria and fungi, and serves to repel insects from particular flowers (Ha et al., 2011; Liu et al., 2012). SA plays an important role in environment, chemical industry and human body, and its detection is also very important.

Herein, we proposed a novel fluorescent switching sensor allowing highly sensitive and selective detection of multiple chemicals of  $Zn^{2+}$  and salicylaldehyde based on BSA protected AuNCs. To impart the fluorescent switching properties of the sensor, SA was interacted with BSA-AuNCs firstly. In this reaction the fluorescence changed from red to green gradually with increasing concentration of SA, which was resulted from the formation of Schiff base with blue-green autofluorescence and quenching of BSA-AuNCs via aggregation. Further added  $Zn^{2+}$  would competitively coordinate with Schiff base ligand, inducing further enhancement of blue fluorescent peak and partial recovery of red fluorescence from BSA-AuNCs. It provides an effective and alternative way for high sensitive and selective detection of zinc ion.

## 2. Material and methods

### 2.1. Materials

Ethanol, chloroauric acid ( $HAuCl_4 \cdot 3H_2O$ ), sodium hydroxide, salicylaldehyde (SA), glutaraldehyde (GA), zinc chloride, formaldehyde, heptanal, paraformaldehyde, benzaldehyde, p-nitrobenzaldehyde, p-dimethylaminobenzaldehyde, cadmium chloride, silver chloride, sodium chloride, aluminum chloride, magnesium chloride, lead chloride, potassium chloride, calcium chloride, chromium chloride, copper chloride, zinc sulfate, zinc acetate and zinc nitrate were purchased from Beijing Chemical Co., China. All chemicals were of analytical reagents and used as received. Bovine serum albumin (BSA) was purchased from Sigma. Fetal bovine serum (FBS) was from Gibco. High purity deionized water ( $18 M\Omega$ ) was produced using a Millipore-Q water system and used in all experiments.

### 2.2. Characterization

Fluorescence measurements were carried out on the Cary Eclipse fluorescence spectrophotometer (Varian, Inc.). The samples for fluorescence measurements were placed in a 10 mm optical path length quartz fluorescence cuvette. UV-vis spectra were recorded using the JASCO V-570 spectrophotometer. Transmission electron microscopy (TEM) was performed on a JEOL JEM 2010F

electron microscope operating at 200 kV.

### 2.3. Synthesis of BSA-AuNCs

BSA-AuNCs were prepared according to previous report with modification (Xie et al., 2009). Briefly, BSA (2 g) was dissolved in deionized water (40 mL) under stirring. Chloroauric acid (40 mL, 10 mmol) was dropwisely added to the solution. After 30 min incubation in 37 °C, the pH of this mixture was adjusted to 12 by adding NaOH (4 mL, 1 mol). Then the bottle was incubated in 37 °C oven for 12 h. Finally, the solution was dialyzed against deionized water for 48 h to completely remove unreacted gold ions.

### 2.4. Detection of SA with BSA-AuNCs

SA with different concentrations was added into 1 mL diluted BSA-AuNCs (2.5 mg mL<sup>-1</sup>). The solution was maintained for 3 min and then the fluorescent spectra were measured. The excitation wavelength was 360 nm and the emission range was 380–800 nm. The excitation and emission slit were 5 nm and 10 nm respectively.

### 2.5. Detection of $Zn^{2+}$ based on the interaction of SA and BSA-AuNCs

Firstly, a final concentration of 0.64 mM SA was added into 1 mL BSA-AuNCs (2.5 mg mL<sup>-1</sup>) and the mixture was maintained for 3 min. Then zinc ion with different concentrations was added into the mixture and kept for 20 min prior to measurement of the fluorescent spectra with an excitation wavelength at 360 nm and an emission range of 380–800 nm. The excitation and emission slit were 5 nm and 10 nm respectively.

### 2.6. Selectivity and anti-interference of detection

To investigate the selectivity of BSA-AuNCs towards salicylaldehyde, aliphatic aldehydes including formaldehyde, glutaraldehyde (GA), heptaldehyde, paraformaldehyde, and some aromatic aldehydes including benzaldehyde, p-nitrobenzaldehyde and p-dimethylaminobenzaldehyde were also detected. To testify the selectivity of BSA-AuNCs (in presence of SA) towards zinc ion, the fluorescence response to other relevant metal ions including alkaline earth ( $Mg^{2+}$ ,  $Ca^{2+}$ ), alkali ( $Na^+$  and  $K^+$ ), transition and heavy metal ions ( $Al^{3+}$ ,  $Pb^{2+}$ ,  $Ag^+$ ,  $Cu^{2+}$ ,  $Cr^{3+}$ ,  $Cd^{2+}$ ) and anions ( $SO_4^{2-}$ ,  $CH_3COO^-$ ,  $Cl^-$  and  $NO_3^-$ ) were also tested and the fluorescence spectra were recorded.

### 2.7. Detection of $Zn^{2+}$ in biological fluid

Standard solution of  $Zn^{2+}$  was prepared by dissolving  $Zn^{2+}$  in biological fluid (FBS was diluted for 10 times with pH 7.4, 0.01 M phosphate buffered saline (PBS)). To detect  $Zn^{2+}$  in the biological fluid, the fluid containing BSA-AuNCs (2.5 mg mL<sup>-1</sup>) and SA (0.64 mM) was equilibrated at room temperature for 3 min. After different concentration of  $Zn^{2+}$  was added in the fluid for 20 min, the fluorescent spectra were recorded.

### 2.8. Data statistics

The calibration curve formula was established according to the relative fluorescence intensity, that is,  $I_1/I_0$ , in which  $I_1$  and  $I_0$  are the maximum emission intensities of the mixture in the presence and absence of SA and/or  $Zn^{2+}$ , respectively. Data are presented as mean  $\pm$  SE (standard error) of three independent experiments.

### 3. Results and discussion

#### 3.1. Design and mechanism of cascade detection of $Zn^{2+}$ and SA using BSA-AuNCs

The fluorescence switching detection of  $Zn^{2+}$  and SA was designed as illustrated in **Scheme 1**. The surface of BSA protected gold nanoclusters is abundant with amino groups. When SA is introduced into the BSA-AuNC suspension, the aldehyde groups of SA can rapidly react with amino groups on BSA-AuNCs and result in the production of imine groups ( $-C=N-$ ) under mild room temperature and aqueous solution, that is the Schiff base reaction to form SA-BSA-AuNC complex (Jia et al., 2012). Schiff base has a weak characteristic peak at about 500 nm (Wu et al., 2007) and the fluorescence intensity depends on the concentration of SA. When the concentration of SA is increased, the fluorescence intensity of Schiff base will enhance. Simultaneously the intrinsic fluorescence from gold nanoclusters with fluorescent peak at 640 nm decreases with increase of SA concentration. When the SA reaches to a high concentration, the fluorescence from BSA-AuNCs can be almost completely quenched. The decrease and quenching of fluorescence from BSA-AuNCs may be attributed to the following reasons. The BSA-AuNCs formed in the BSA solution are stabilized by the formation of Au-S bond of Au with the protein (via the 35 cysteine residues in BSA) as template and the steric protection due to the bulkiness of the protein (Xie et al., 2009). So the fluorescence of BSA-AuNCs is highly dependent on the BSA's protection. When SA is introduced into BSA-AuNCs, the aldehyde groups of SA can rapidly react with amino groups of BSA to form imine groups ( $C=N$ ) (Gharagozlou and Boghei, 2012) and change the surface state of the BSA template. The AuNCs lose the protection of BSA ligands, and then the aggregation of BSA-AuNCs occurs and the fluorescence is quenched. To verify the mechanism, we also included other parameters like pH and ionic strength that might possibly influence the fluorescence of AuNCs. As shown in **Fig. S5**, pH and ionic strength would not induce obvious fluorescence change and aggregation of BSA-AuNCs. The obtained results were consistent with previous reports (Liu et al., 2013). The spherical nanoaggregates from BSA-AuNCs in presence of SA with polydispersed size were confirmed by TEM (**Fig. S1a** in the Supplemental material).

$Zn^{2+}$  is further introduced into the system with pre-formed SA-BSA-AuNC complex in the second step. There is a strong coordination interaction among  $Zn^{2+}$ , the  $C=N$  of Schiff base and the hydroxyl groups of SA. This interaction will weaken the

electron-donating ability of the hydroxyl groups of SA, then reducing the charge transfer efficiency in the system, will cause a final blue-shift of the fluorescence peak of Schiff base from 500 nm to 446 nm (Xu et al., 2005). Meanwhile, due to the complexation of  $Zn^{2+}$ , the isomerization of  $C=N$  will be strongly inhibited, thus enhancing the fluorescence intensity at 500 nm (Wu et al., 2007). Meantime, there is a strong coordination interaction among  $Zn^{2+}$ , the  $C=N$  of Schiff base and the hydroxyl groups of SA. This strong coordination will reduce the interaction between SA and BSA-AuNCs, and partially release the BSA-AuNCs from aggregation. The nanoaggregates became more incompact and some isolated gold nanoclusters were found from TEM (red arrow in **Fig. S1b** in the Supplemental materials). Totally, the new-arisen blue-green fluorescent peak together with the reversible change of fluorescent intensity of BSA-AuNCs contributes to the fluorescence switching method for SA and  $Zn^{2+}$  detection with high sensitivity and high selectivity.

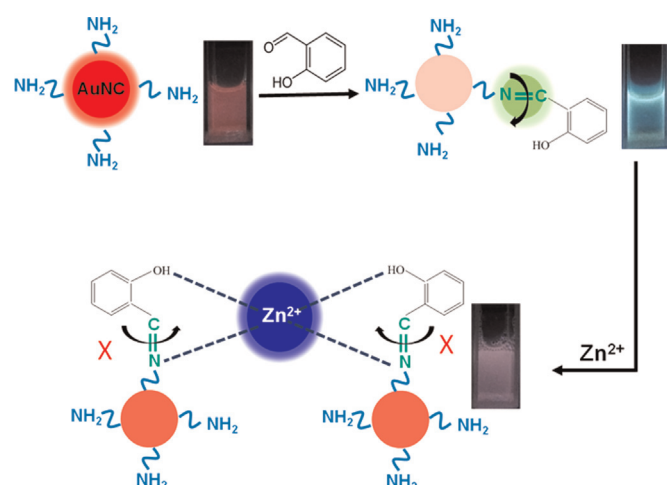
#### 3.2. Characterization of BSA-AuNCs

The size of BSA-AuNCs was about 2–3 nm with uniform size and good dispersibility (**Fig. S2a**). Under visible and 365 nm UV light, the dispersion had brown color and bright red fluorescence, respectively (**Fig. S2b and c**). **Fig. S2d** shows the UV-visible absorbance, fluorescent excitation and emission spectra of the nanoclusters. It showed emission peaks at 640 nm with a full width at half-maximum (FWHM) of 111 nm. In the excitation spectrum, three separate peaks were observed at 257 nm, 320 nm and 495 nm. In the UV-visible absorbance spectrum, there was an absorption peaks at 280 nm, which was attributed from the characteristic absorption of tryptophan in BSA. No characteristic absorption peak appeared at the range of visible light, indicating that no plasmonic gold particles were formed.

#### 3.3. SA detection using BSA-AuNCs as fluorescent probes

For sensing SA, fluorescent spectra were recorded after incubating SA with BSA-AuNCs for 3 min. The fluorescent spectra had no obvious change with prolonged time (data not shown). A broad SA concentration from 1.6  $\mu$ M to 3.15 mM was detected. After adding SA, a new individual fluorescent peak appeared that was centered at 500 nm. With the increase of SA concentration from 1.6  $\mu$ M to 3.15 mM, there had a decrease of the fluorescence at 640 nm (intrinsic fluorescence from BSA-AuNCs) and a contrary increase of the fluorescent peak at 500 nm (**Fig. 1a**). About 7.5 fold fluorescence enhancement at 500 nm and more than 80% fluorescence decrease at 640 nm was observed respectively when the concentration of SA reached 3.15 mM. At a low SA concentration of 7.8  $\mu$ M, fluorescent change could be clearly observed. From the fluorescence change under UV light illumination ( $\lambda_{ex}=365$  nm), the color showed a gradual change from red, to orange, and then to green, which was a mixed color from the fluorescence peak at 500 nm and 640 nm (**Fig. 1b**).

The relative fluorescence intensity  $I_1/I_0$  ( $I_1$  and  $I_0$  are the fluorescence intensity in presence and absence of SA respectively) at the emission wavelength of 500 nm and 640 nm versus the SA concentration was plotted respectively (**Fig. 1c and d**). At 500 nm, the presence of trace amounts of SA resulted in a visible enhancement of the emission at 500 nm. The resulting plot, that was shown in the inset of **Fig. 1b**, displayed a good linear relationship within the SA concentration range from 0  $\mu$ M to 0.16 mM with a linear correlation  $R^2=0.998$ . In comparison, trace amounts of SA induced a decrease of fluorescence at 640 nm. It showed a good linear relationship in the SA concentration range from 15.8  $\mu$ M to 1.58 mM with a linear correlation  $R^2=0.987$ . Following the IUPAC (International Union of Pure and Applied Chemistry) criterion, the



**Scheme 1.** Schematic illustration of the fluorescence switching strategy for detection of SA and  $Zn^{2+}$ .

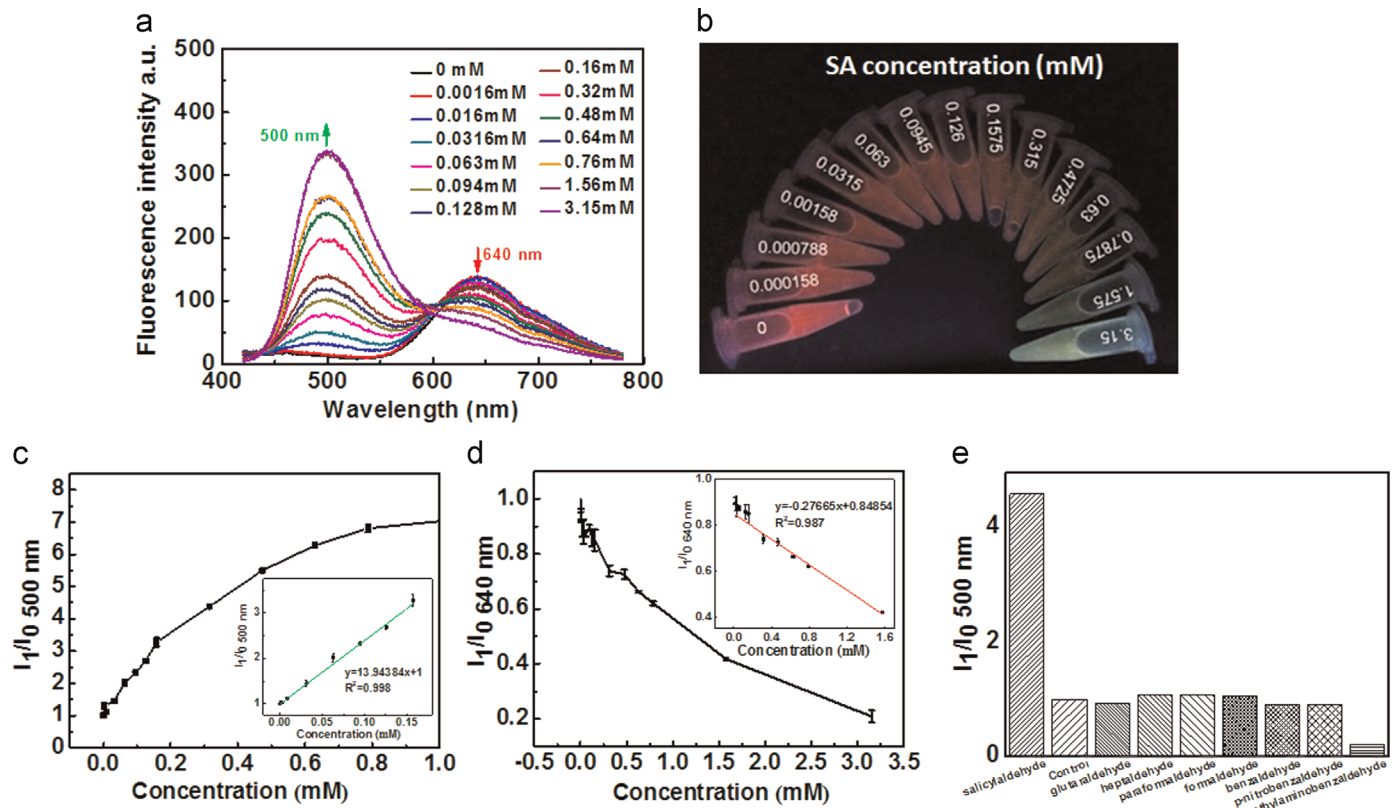


**Fig. 1.** (a) The emission spectra of BSA-AuNCs in the presence of different concentrations of SA and (b) corresponding photographic image of the samples under UV lamp irradiation ( $\lambda_{\text{ex}}=365 \text{ nm}$ ). Concentration–response curve at fluorescent peak of (c) 500 and (d) 640 nm, respectively. The insets show the plot of the relative fluorescence intensity ( $I_1/I_0$ ) recorded at 500 nm and 640 nm fluorescent peaks versus the concentration of SA resulting from Stern–Volmer analysis respectively. (e) The fluorescence response of  $I_1/I_0$  500 nm in the presence of 0.64 mM aldehydes.

limit of detection (LOD) was calculated to be  $0.19 \mu\text{M}$  at 500 nm and  $1.99 \mu\text{M}$  at 640 nm respectively, based on  $3 \times \text{SD}/S$ , in which SD is the standard deviation of the intercept and S is the slope of the calibration curve. Compared with the detection from fluorescent change of single peak, the simultaneous fluorescent change at two fluorescence peak at 500 nm and 640 nm, both with good linear relationship versus the SA concentration, greatly increased the detection accuracy and decreased the lowest detection limit.

To test the selectivity of this fluorescence changing behavior toward SA, several other aldehydes were also investigated. The relative fluorescence intensity variation at 500 nm ( $I_1/I_0$  500 nm) against aliphatic aldehydes including formaldehyde, glutaraldehyde (GA), heptaldehyde, paraformaldehyde, and some aromatic aldehydes including benzaldehyde, p-nitrobenzaldehyde and p-dimethylaminobenzaldehyde are shown in Fig. 1e. Under the same concentration, no fluorescence enhancement at 500 nm was observed upon the adding the above aldehydes. This result suggested high selectivity of the fluorescence switching strategy toward SA.

#### 3.4. $\text{Zn}^{2+}$ detection via BSA-AuNCs in presence of SA

To examine the feasibility of using the fluorescent switching sensing probes for  $\text{Zn}^{(II)}$  detection, zinc chloride with different concentrations was added into the mixture of BSA-AuNCs and SA (0.64 mM) after the fluorescence was stable, and the fluorescence spectra were monitored. We also tested the effect of concentration of SA towards the detection of  $\text{Zn}^{2+}$ . As shown in Fig. S6, only when the concentration of SA was 0.64 mM, we could get the obvious change in 446 nm and 640 nm simultaneously. Fig. 2a presents the fluorescence emission spectra with different  $\text{Zn}^{2+}$

concentrations from  $0.1 \mu\text{M}$  to  $100 \mu\text{M}$ . With the increase of  $\text{Zn}^{2+}$  concentration, the maximum emissive wavelength shifted from 500 nm to 446 nm and the fluorescent intensity enhanced obviously with increase of  $\text{Zn}^{2+}$  concentration. Meanwhile, the fluorescent peak at 640 nm of the intrinsic fluorescence from BSA-AuNCs recovered partially. Combining the fluorescent change of peak at 446 nm and 640 nm, the relative fluorescence intensity  $I_1/I_0$  446 nm at 446 nm and  $I_1/I_0$  640 nm at 640 nm were calculated versus the  $\text{Zn}^{2+}$  concentration (Fig. 2b and c). At 446 nm, the plot displayed a good linear relationship in a broad  $\text{Zn}^{2+}$  concentration range from  $0 \mu\text{M}$  to  $100 \mu\text{M}$  with a linear correlation  $R^2=0.992$  (Fig. 2b). Similarly, a broad  $\text{Zn}^{2+}$  concentration range from  $0 \mu\text{M}$  to  $90 \mu\text{M}$  with a linear correlation  $R^2=0.995$  was calculated at 640 nm (Fig. 2c). The limit of  $\text{Zn}^{2+}$  detection was also calculated, following the IUPAC criterion, and the result showed the lowest detection limit as low as  $29.28 \text{ nM}$  (from the formula at 446 nm), which was far lower than previous reports (Kim, K.B., et al., 2013; Shahid et al., 2012; Wang et al., 2013). It was also far below the guidelines of the WHO for drinking water ( $76 \mu\text{M}$ ), and the physiological content in human serum ( $10 \mu\text{M}$ ). This result demonstrates that this new detection method can match the requirement of assaying  $\text{Zn}^{2+}$ . Under a 365 nm UV light irradiation, a fluorescent color change from orange to lavender could be directly observed with increase of  $\text{Zn}^{2+}$  concentration, which was overlaid from the fluorescence in the region of purple–blue and red fluorescence (Fig. 2d). It should be noted that when  $\text{Zn}^{2+}$  was added into BSA-AuNCs in absence of SA (Fig. S3a in Supplementary materials) and SA in absence of BSA-AuNCs (Fig. S3b in Supplementary materials) respectively, the fluorescence change was not obvious, demonstrating a cross-interaction among the three kinds of substance.

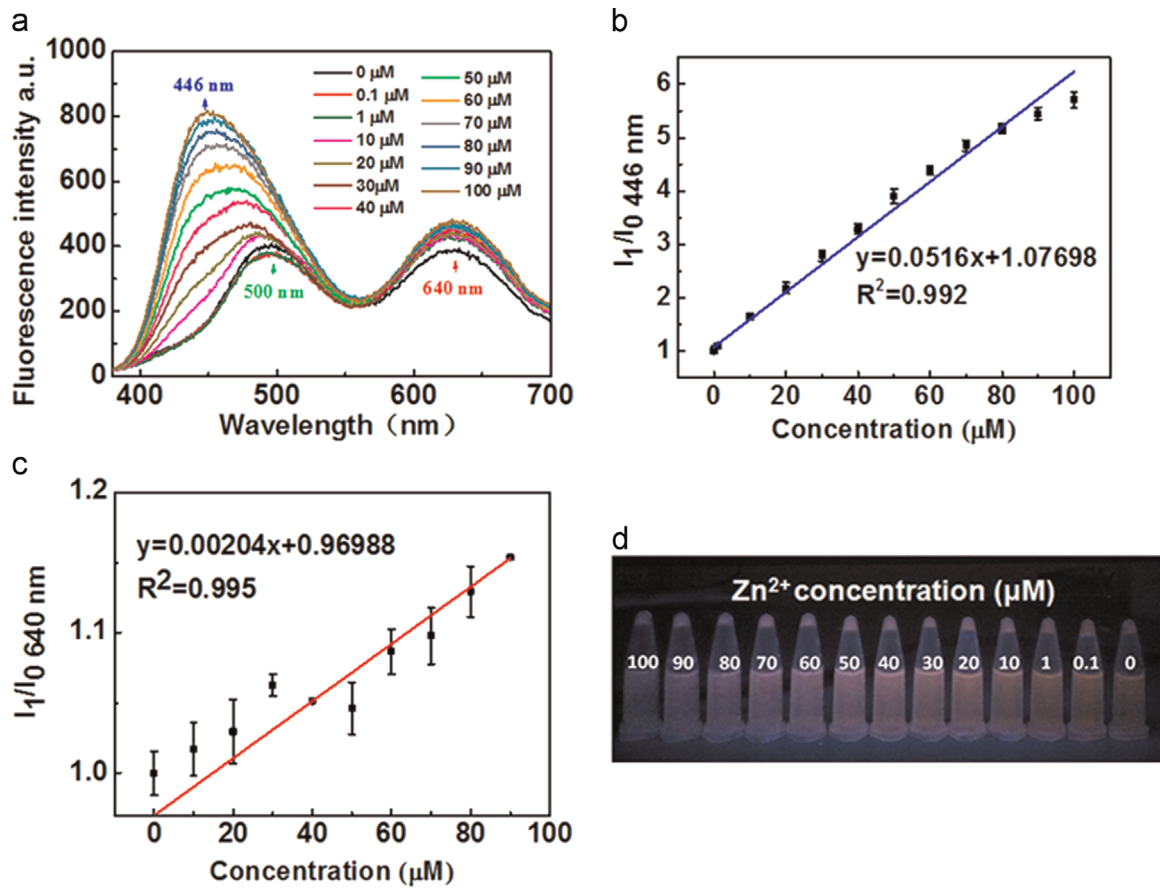


**Fig. 2.** (a) The fluorescence emission spectra of BSA-AuNCs in the presence of 0.64 mM SA with different concentrations of  $Zn^{2+}$ , (b, c) the plot of the relative fluorescence intensity ( $I_1/I_0$ ) recorded at (b) 446 nm and (c) 640 nm fluorescent peaks versus the concentration of  $Zn^{2+}$  resulting from Stern-Volmer analysis respectively. (d) Corresponding photographic images of the samples under UV lamp irradiation ( $\lambda_{ex}=365$  nm).

### 3.5. Selectivity and practical detection of $Zn^{2+}$

We also investigated the selectivity of the fluorescence switching behavior for detecting  $Zn^{2+}$  using BSA-AuNCs in presence of SA. The response of BSA-AuNCs in presence of SA upon addition of  $Zn^{2+}$  and some other metal cations including  $Cu^{2+}$ ,  $Cd^{2+}$ ,  $Cr^{3+}$ ,  $Na^+$ ,  $Pb^{2+}$ ,  $Ag^+$ ,  $Mg^{2+}$ ,  $Al^{3+}$ ,  $Ca^{2+}$  and  $K^+$  was monitored. Under the same cation concentration, no obvious fluorescence change at 446 nm and 640 nm was observed upon the adding of these possible coexisting metal cations. The relative fluorescence intensity variation ( $I_1/I_0$ ) at 446 nm had a change only in presence of  $Zn^{2+}$  (Fig. 3). For the fluorescent color of the detecting solution, it turned from orange to pink and then to purple with the increase of  $Zn^{2+}$  concentration. But the solution with adding of other cations had no obvious change of fluorescent color (Fig. 3, inset). This result suggested high selectivity of the fluorescence switching strategy toward  $Zn^{2+}$ . It is known that the chelating groups of  $-C=N-$  exhibit a high affinity toward transition and post-transition metal cations, but less binding affinity toward alkali metal and alkaline earth metal cations due to their different electronic structures.  $Zn^{2+}$  has extraordinarily high response in fluorescence spectrum instead of other metal cations, enabling high sensitive and selective detection. In addition, when other zinc salts (anions as  $SO_4^{2-}$ ,  $CH_3COO^-$ ,  $Cl^-$  and  $NO_3^-$ ) instead of  $ZnCl_2$  were used for the detection, the fluorescence of BSA-AuNCs in presence of SA had similar response with that of  $ZnCl_2$  that the fluorescent peak at 446 nm increased along with the fluorescence recovery of BSA-AuNCs at 640 nm. The  $I_1/I_0$  at 446 nm has similar value of these for  $Zn^{2+}$  salt solution (Fig. S4 in Supplementary material). These results confirmed the high

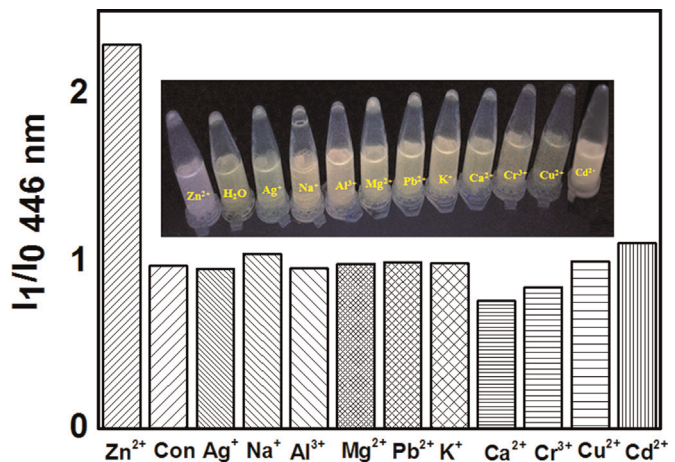


**Fig. 3.** The fluorescence response of BSA-AuNCs in the presence of SA upon 60  $\mu$ M metal ions and corresponding photographic images of the samples under UV lamp irradiation ( $\lambda_{ex}=365$  nm).

selectivity of the proposed fluorescence switching method for  $Zn^{2+}$  detection.

The applicability of this fluorescence switching detection of  $Zn$  (II) for the assay of practical samples was further evaluated. Fetal bovine serum was diluted with PBS buffer for 10 times. Fig. 4 shows the fluorescence emission spectra, the linear plot and photographs of the mixtures with different concentrations of  $Zn^{2+}$ . Similar with  $Zn^{2+}$  detection in water, there was an obvious increase of fluorescence intensity at 446 nm, displaying a good

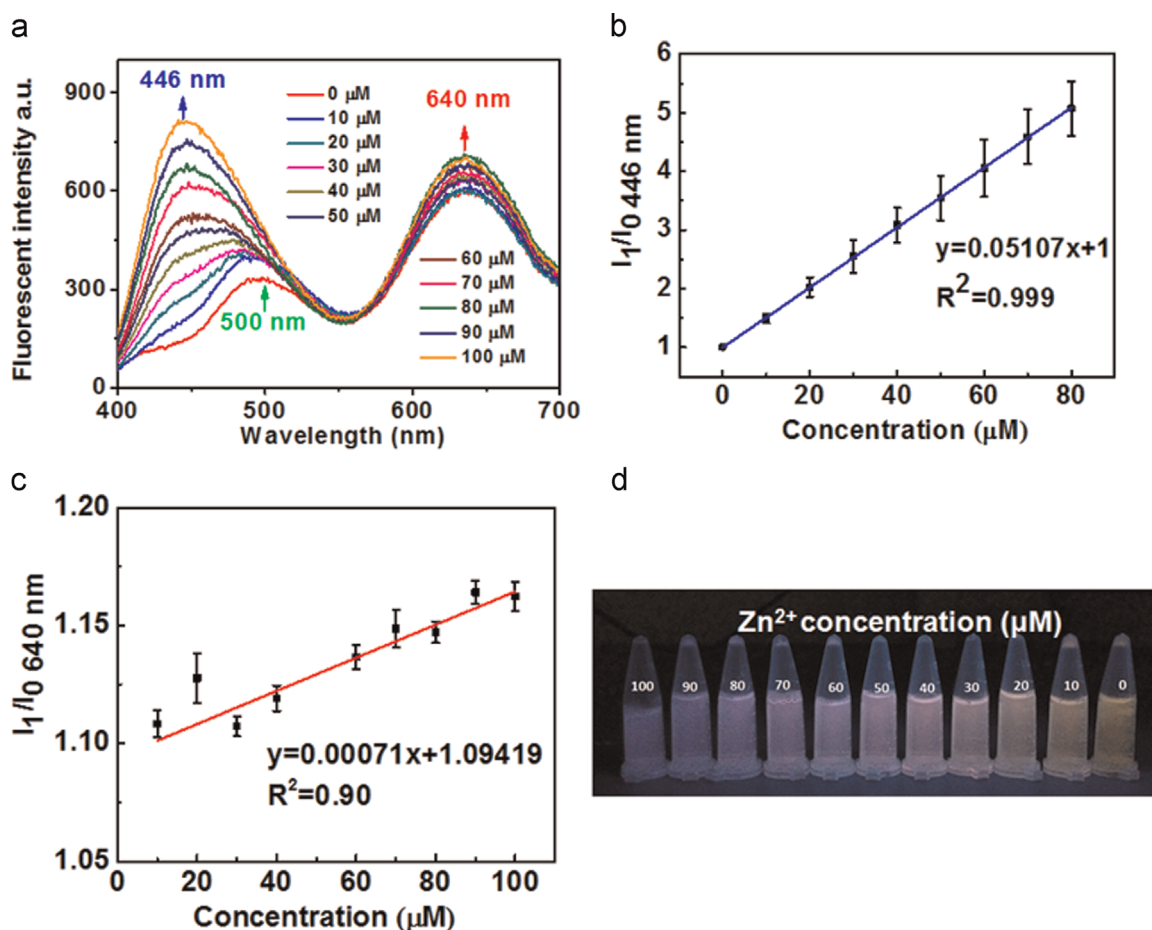


**Fig. 4.** (a) The fluorescence emission spectra of BSA-AuNCs in the presence of 0.64 mM SA with different concentrations of  $Zn^{2+}$  in PBS diluted FBS. (b, c) The plot of the relative fluorescence intensity ( $I_1/I_0$ ) recorded at (b) 446 nm and (c) 640 nm fluorescent peaks versus the concentration of  $Zn^{2+}$  resulting from Stern-Volmer analysis respectively. (d) Corresponding photographic images of the samples under UV lamp irradiation ( $\lambda_{ex}=365$  nm).

**Table 1**  
Recoveries of  $Zn^{2+}$  in practical samples detected by the fluorescence switching method.

Sample	Supplemented ( $\mu M$ )	Measured ( $\mu M$ )	Recovery (%)	RSD (%)
PBS containing 10% FBS	20	20.12	100.58	0.279
	50	49.84	99.67	0.259
	80	79.71	99.63	0.196

linear relationship in the range of 10–80  $\mu M$  ( $R^2=0.999$ ) (Fig. 4b). The limit of detection was also calculated to be as low as 80 nM, following the IUPAC criterion. An increase of fluorescence was also observed at 640 nm with linear relationship in the range of 10–100  $\mu M$  ( $R^2=0.90$ ). Under 365 nm UV light irradiation, the color was changed from orange to lavender with increase of  $Zn^{2+}$  concentration. Standard recovery experiments were carried out in diluted FBS. As listed in Table 1, the recoveries of 20, 50, 80  $\mu M$   $Zn^{2+}$  were 99.63%, 99.67% and 100.58% respectively. It proved that there was little interference of substrates in the serum. Therefore, the developed method had good performance in practical detections of  $Zn^{2+}$  in real samples.

#### 4. Conclusions

In conclusion, we have developed a new fluorescence switching

sensor for cascade detection of multiple chemicals of  $Zn^{2+}$  and salicylaldehyde (SA) based on BSA-AuNCs. The fluorescent switching behaviors were based on formation of Schiff base between amino groups of BSA-AuNCs and aldehyde groups of SA and competitive binding of  $Zn^{2+}$  with the Schiff base to form complexing agents, along with the reversible aggregation behavior of gold nanoclusters. The new fluorescence switching sensor for  $Zn^{2+}$  have advantages of simplicity, rapidity, naked-eye detection, high sensitivity and selectivity. This work may provide an alternative way to detect  $Zn^{2+}$  in practice, and expand the application of the protein protected gold nanoclusters in biosensor.

#### Acknowledgments

We acknowledge financial support from the National Natural Science Foundation of China, China (Project nos. 31270022, 81471784, and 31271075).

#### Appendix A. Supplementary information

Supplementary data associated with this article can be found in the online version at <http://dx.doi.org/10.1016/j.bios.2015.06.034>.

## References

- Adhikari, B., Banerjee, A., 2010. *J. Mater. Chem.* 22, 4364–4371.
- Albrecht, M.R., Cid, C., Faugère, J.-C., Perret, L., 2012. *J. Symb. Comput.* 47, 926–941.
- Chen, W., Tu, X., Guo, X., 2009. *Chem. Commun.*, 1736–1738.
- Chen, X., Nam, S.W., Jou, M.J., Kim, Y., Kim, S.J., Park, S., Yoon, J., 2008. *Org. Lett.* 10, 5235–5238.
- Chen, X., Zhou, Y., Peng, X., Yoon, J., 2010. *Chem. Soc. Rev.* 39, 2120–2135.
- Cozzi, P.G., 2004. *Chem. Soc. Rev.* 33, 410–421.
- Diez, I., Ras, R.H., 2011. *Nanoscale* 3, 1963–1970.
- Ding, Y., Xie, Y., Li, X., Hill, J.P., Zhang, W., Zhu, W., 2011. *Chem. Commun.* 47, 5431.
- Gupta, V.K., Singh, A.K., Ganjali, M.R., Norouzi, P., Faribod, F., Mergu, N., 2013. *Sensors Actuat. B – Chem.* 182, 642–651.
- Ha, Y., Liew, H., Park, H.Y., Kim, K., Suh, Y.H., Churchill, D.G., 2011. *J. Neurosci. Res.* 712, 168–177.
- Huang, Y., Lin, Q., Wu, J., Fu, N., 2013. *Dyes Pigment.* 99, 699–704.
- Jia, Y., Cui, Y., Fei, J., Du, M., Dai, L., Li, J., Yang, Y., 2012. *Adv. Funct. Mater.* 22, 1446–1453.
- Jiang, J., Jiang, H., Tang, X., Yang, L., Dou, W., Liu, W., Fang, R., Liu, W., 2011. *Dalton Trans.* 40, 6367–6370.
- Jiang, X., Sun, C., Guo, Y., Nie, G., Xu, L., 2015. *Biosens. Bioelectron.* 64, 165–170.
- Joseph, R., Chinta, J.P., Rao, C.P., 2010. *J. Org. Chem.* 75, 3387–3395.
- Jung, H.S., Kwon, P.S., Lee, J.W., Kim, J.I., Hong, C.S., Kim, J.W., Yan, S.H., Lee, J.Y., Lee, J.H., Joo, T., Kim, J.S., 2009. *J. Am. Chem. Soc.* 131, 2008–2012.
- Kim, J.H., Noh, J.Y., Hwang, I.H., Kang, J., Kim, J., Kim, C., 2013a. *Tetrahedron Lett.* 54, 2415–2418.
- Kim, K.B., Kim, H., Song, E.J., Kim, S., Noh, I., Kim, C., 2013b. *Dalton Trans.* 42, 16569–16577.
- Lee, H.G., Lee, J.H., Jang, S.P., Park, H.M., Kim, S.J., Kim, Y., Kim, C., Harrison, R.G., 2011. *Tetrahedron* 67, 8073–8078.
- Lee, J.W., Choi, S.-P., Thiruvenkatachari, R., Shim, W.-G., Moon, H., 2006. *Dyes Pigment.* 69, 196–203.
- Lee, J.A., Eom, G.H., Park, H.M., Lee, J.H., Song, H., Hong, C.S., Yoon, S., Kim, C., 2012. *Bull. Korean Chem. Soc.* 33, 3625–3628.
- Liu, H.Y., Yang, G.H., Abdel-Halim, E.S., Zhu, J.-J., 2013. *Talanta* 104, 135–139.
- Lin, Y.H., Tseng, W.L., 2010. *Anal. Chem.* 82, 9194–9200.
- Liu, M., Deng, J., Lai, C., Chen, Q., Zhao, Q., Zhang, Y., Li, H., Yao, S., 2012. *Talanta* 100, 229–238.
- Liu, Z., Zhang, C., Li, Y., Wu, Z., Qian, F., Yang, X., He, W., Gao, X., Guo, Z., 2009. *Org. Lett.* 11, 795–798.
- Maity, D., Govindaraju, T., 2012. *Chem. Commun.* 48, 1039–1041.
- Gharagozlou, M., Boghaei, D.M., 2012. *Spectrochim. Acta A* 71, 1617–1622.
- Park, H.M., Oh, B.N., Kim, J.H., Qiong, W., Hwang, I.H., Jung, K.-D., Kim, C., Kim, J., 2011. *Tetrahedron Lett.* 52, 5581–5584.
- Santhosh, M., Chinnadayyala, S.R., Kakoti, A., Goswami, P., 2014. *Biosens. Bioelectron.* 59, 370–376.
- Shahid, M., Srivastava, P., Razi, S.S., Ali, R., Misra, A., 2012. *J. Incl. Phenom. Macrocycl.* 77, 241–248.
- Sheng, R., Wang, P., Gao, Y., Wu, Y., Liu, W., Ma, J., Li, H., Wu, S., 2008. *Org. Lett.* 10, 5015–5018.
- Swamy, K.M.K., Kim, M.-J., Jeon, H.-R., Jung, J.-Y., Yoon, J.-Y., 2010. *Bull. Korean Chem. Soc.* 31, 3611–3616.
- Takeda, A., 2001. *Biometals* 14, 343–351.
- Tu, X., Chen, W., Guo, X., 2011. *Nanotechnology* 22, 095701.
- Wang, H., Sun, C.L., Yue, Y.H., Yin, F.F., Jiang, J.Q., Wu, H.R., Zhang, H.L., 2013. *Analyst* 138, 5576–5579.
- Wu, J.S., Liu, W.M., Zhuang, X.Q., Wang, F., Wang, P.F., Tao, S.L., Zhang, X.H., Wu, S.K., Lee, S.T., 2007. *Org. Lett.* 9, 33–36.
- Xie, J., Zheng, Y., Ying, J.Y., 2009. *J. Am. Chem. Soc.* 131, 888–889.
- Xie, J., Zheng, Y., Ying, J.Y., 2010. *Chem. Commun.* 46, 961–963.
- Xu, H., Suslick, K.S., 2010. *Adv. Mater.* 22, 1078–1082.
- Xu, Y., Meng, J., Meng, L., Dong, Y., Cheng, Y., Zhu, C., 2010. *Chemistry – Eur. J.* 16, 12898–12903.
- Xu, Z.C., Xiao, Y., Qian, X.H., Cui, J.N., Cui, D.W., 2005. *Org. Lett.* 7, 889–892.
- Zheng, J., Nicovich, P.R., Dickson, R.M., 2007. *Annu. Rev. Phys. Chem.* 58, 409–431.
- Zhou, Y., Jung, J.Y., Jeon, H.R., Kim, Y., Kim, S.J., Yoon, J., 2011. *Org. Lett.* 13, 2742–2745.